Representation Learning Dynamics of Self-Supervised Models

Anonymous authors
Paper under double-blind review

Abstract

Self-Supervised Learning (SSL) is an important paradigm for learning representations from unlabelled data, and SSL with neural networks has been highly successful in practice. However current theoretical analysis of SSL is mostly restricted to generalisation error bounds. In contrast, learning dynamics often provide a precise characterisation of the behaviour of neural networks based models but, so far, are mainly known in supervised settings. In this paper, we study the learning dynamics of SSL models, specifically representations obtained by minimising contrastive and non-contrastive losses. We show that a näive extension of the dymanics of multivariate regression to SSL leads to learning trivial scalar representations that demonstrates dimension collapse in SSL. Consequently, we formulate SSL objectives with orthogonality constraints on the weights, and derive the exact (network width independent) learning dynamics of the SSL models trained using gradient descent on the Grassmannian manifold. We also argue that the infinite width approximation of SSL models significantly deviate from the neural tangent kernel approximations of supervised models. We numerically illustrate the validity of our theoretical findings, and discuss how the presented results provide a framework for further theoretical analysis of contrastive and non-contrastive SSL.

1 Introduction

A common way to distinguish between learning approaches is to categorize them into unsupervised learning, which relies on a input data consisting of a feature vector (x), and supervised learning which relies on feature vectors and corresponding labels (x, y). However, in recent years, Self-Supervised Learning (SSL) has been established as an important paradigm between supervised and unsupervised learning as it does not require explicit labels but relies on implicit knowledge of what makes some samples semantically close to others. Therefore SSL builds on inputs and inter-sample relations (x, x^+), where x^+ is often constructed through data-augmentations of x known to preserve input semantics such as additive noise or horizontal flip for an image Kanazawa et al. (2016); Novotny et al. (2018); Gidaris et al. (2018). While the idea of SSL is not new Bromley et al. (1993), recent deep SSL models have been highly successful in computer vision Chen et al. (2020); Caron et al. (2021); Jing & Tian (2019), natural language processing Misra & Maaten (2020); Devlin et al. (2019), speech recognition Steffen et al. (2019); Mohamed et al. (2022). Since the early works Bromley et al. (1993), methods for SSL have predominantly relied on neural networks however with a strong focus on model design with only little theoretical backing.

The main focus of the theory literature on SSL has been either on providing generalization error bounds for downstream tasks on embeddings obtained by SSL (Arora et al., 2019b; Ge et al., 2023; Bansal et al., 2021; Lee et al., 2021; Saunshi et al., 2021; Tosh et al., 2021; Wei et al., 2021; Bao et al., 2022; Chen et al., 2022), or analysing the spectral and isoperimetric properties of data augmentation (Balestriero & LeCun, 2022; Han et al., 2023; Zhuo et al., 2023). The latter approach also result in novel bounds on the generalisation error (HaoChen et al., 2021; Zhai et al., 2023). While generalisation theory remains one of the fundamental tools to characterise the statistical performance, it has been already established for supervised learning that classical generalisation error bounds do not provide a complete theoretical understanding and can become trivial in the context of neural network models (Zhang et al., 2017; Neyshabur et al., 2017). Therefore a

key focus in modern deep learning theory is to understand the learning dynamics of models, often under gradient descent, as they provide a more tractable expression of the problem that can be an essential tool to understand the loss landscape and convergence (Fukumizu, 1998; Saxe et al., 2014; Pretorius et al., 2018), early stopping (Li et al., 2021), linearised (kernel) approximations (Jacot et al., 2018; Du et al., 2019) and, mostly importantly, generalisation and inductive biases (Soudry et al., 2018; Luo et al., 2019; Heckel & Yilmaz, 2021).

In this paper, we analyze the learning dynamics of SSL models under contrastive and non-contrastive losses (Arora et al., 2019b; Chen et al., 2020), which we show to be significantly different from the dynamics of supervised models. This gives a simple and precise characterization of the dynamics that can provide the foundation for future theoretical analysis of SSL models. Before presenting the learning dynamics, we recall the SSL principles and losses consisdered in this work.

Contrastive Learning. Contrastive SSL has its roots in the work of Bromley et al. (1993). Recent deep learning based contrastive SSL show great empirical success in computer vision (Chen et al., 2020; Caron et al., 2021; Jing & Tian, 2019), video data (Fernando et al., 2017; Sermanet et al., 2018), natural language tasks (Misra & Maaten, 2020; Devlin et al., 2019) and speech (Steffen et al., 2019; Mohamed et al., 2022). In general a contrastive loss is defined by considering an anchor image, $x \in \mathbb{R}^d$, positive samples $\{x^+\} \subset \mathbb{R}^d$ generated using data augmentation techniques as well as independent negative samples $\{x^-\} \subset \mathbb{R}^d$. The heuristic goal is to align the anchor more with the positive samples than the negative ones, which is rooted in the idea of maximizing mutual information between similar samples of the data. In this work, we consider a simple contrastive loss minimisation problem along the lines of Arora et al. (2019b), assuming exactly one positive sample x_i^+ and one negative sample x_i^- for each anchor x_i,[1]

$$\min_{\Theta} \sum_{i=1}^{n} u(x_i)^\top \left(u(x_i^-) - u(x_i^+) \right), \tag{1}$$

where $u = [u_1(\cdot, \Theta) \dots u_z(\cdot, \Theta)]^\top : \mathbb{R}^d \to \mathbb{R}^z$ is the embedding function, parameterized by Θ, the learnable parameters.

Non-Contrastive Learning Non-contrastive losses emerged from the observation that negative samples (or pairs) in contrastive SSL are not necessary in practice, and it suffices to maximise only alignment between positve pairs Chen & He (2021); Chen et al. (2020); Grill et al. (2020). Considering a simplified version of the setup in Chen et al. (2020) one learns a representation by minimising the loss [2]

$$\min_{\Theta} \sum_{i=1}^{n} -u(x_i)^\top u(x_i^+). \tag{2}$$

The embedding $u = [u_1(\cdot, \Theta) \dots u_z(\cdot, \Theta)]^\top : \mathbb{R}^d \to \mathbb{R}^z$, parametrised by Θ, typically comprises of a base encoder network and a projection head in practice (Chen et al., 2020).

Contributions. The objective of this paper is to derive the evolution dynamics of the learned embedding $u = u(\cdot, \theta)$ under gradient flow for the constrastive (1) and non-contrastive losses (2). More specifically we show the following:

- We express the learning dynamics for both contrastive and non-contrastive learning and show that, the evolution dynamics is same across dimensions. This explains why SSL is naturally prone to dimension collapse.
- Assuming a 2-layer linear network, we show that dimension collapse cannot be avoided by adding standard Frobenius norm reguralisation or constraint, but by adding orthogonality or L2 norm constraints.

[1] It is straightforward to extend our analysis to multiple positive and negative samples, but the expressions become cumbersome, without providing additional insights.

[2] We simplify Chen et al. (2020) by replacing the cosine similarity with the standard dot product and also by replacing an additional positive sample x_i^{++} by anchor x_i for convenience.

- We further show that at initialization, the dynamics of 2-layer network with nonlinear activation is close to their linear, width independent counterparts (Theorem 1). We also provide empirical evidence that the evolution of the infinite width non-linear networks are close to their linear counterparts, under certain conditions on the nonlinearity (that hold for tanh).

- We derive the learning dynamics of SSL for linear networks, under orthogonality constraints (Theorem 2). We further show the convergence of the learning dynamics for the one dimensional embeddings ($z = 1$).

- We numerically show, on the MNIST dataset, that our derived SSL learning dynamics can be solved significantly faster than training nonlinear networks, and yet provide comparable accuracy on downstream tasks.

All proofs are provided in the supplementary material.

Related works. Our focus is on the evolution of the learned representations, and hence, considerably different from the aforementioned literature on generalisation theory and spectral analysis of SSL. From an optimisation perspective, Liu et al. (2023) derive the loss landscape of contrastive SSL with linear models, $u(x) = Wx$, under InfoNCE loss van den Oord et al. (2018). Although the contrastive loss in (1) seems simpler than InfoNCE, they are structurally similar under linear models (Liu et al., 2023, see Eqns. 4–6). Training dynamics for contrastive SSL with deep linear models have been partially investigated by Tian (2022), who show an equivalence with principal component analysis, and by Jing et al. (2022), who establish that dimension collapse occurs for over-parametrised linear contrastive models. Theorem 2 provides a more precise characterisation and convergence criterion of the evolution dynamics than previous works. Furthermore, none of prior works consider non-linear models or orthogonality constraints as studied in this work.

We also distinguish our contributions (and discussions on neural tangent kernel connections) with the kernel equivalents of SSL studied in Kiani et al. (2022); Johnson et al. (2023); Shah et al. (2022); Cabannes et al. (2023). While Shah et al. (2022); Cabannes et al. (2023) specifically pose SSL objectives using kernel models, Kiani et al. (2022); Johnson et al. (2023) show that contrastive SSL objectives induce specific kernels. Importantly, these works neither study the learning dynamics nor consider the neural tangent kernel regime.

Notation. Let $\mathbb{I}_n$ be an $n \times n$ identity matrix. For a matrix A let $\|A\|_F$ and $\|A\|_2$ be the standard frobenious norm and the $L2$-operator norm respectively. The machine output is denoted by $u(\cdot)$. While u is time dependent and should be more accurately denoted as u_t we suppress the subscript where obvious. For any time dependent function, for instance u, denote $\mathring{u}$ to be its time derivative i.e. $\frac{du_t}{dt}$. ϕ is used to denote our non-linear activation function and we abuse notation to also denote its co-ordinate-wise application on a vector by $\phi(\cdot)$. $\langle \cdot, \cdot \rangle$ is used to denote the standard dot product.

2 Learning Dynamics of Regression and its Näive Extension to SSL

In the context of regression, Jacot et al. (2018) show that the evolution dynamics of (infinite width) neural networks, trained using gradient descent under a squared loss, is equivalent to that of specific kernel machines, known as the neural tangent kernels (NTK). The analysis has been extended to a wide range of models, including convolutional networks (Arora et al., 2019a), recurrent networks (Alemohammad et al., 2021), overparametrised autoencoders (Nguyen et al., 2021), graph neural networks (Du et al., 2019; Sabanayagam et al., 2022) among others. However, these works are mostly restricted to squared losses, with few results for margin loss (Chen et al., 2021), but derivation of such kernel machines are still open for contrastive or non-contrastive losses (1)–(2), or broadly, in the context of SSL. To illustrate the differences between regression and SSL, we outline the learning dynamics of multivariate regression with squared loss, and discuss how a näive extension to SSL is inadequate.

2.1 Learning Dynamics of Multivariate Regression

Given a training feature matrix $X := [x_1, \cdots, x_n]^\top \in \mathbb{R}^{n\times d}$ and corresponding z-dimensional labels $Y := [y_1, \cdots, y_n]^\top \in \mathbb{R}^{n\times z}$, consider the regression problem of learning a neural network function $u(x) = [u_1(x, \Theta) \dots u_z(x, \Theta)]^\top$, parameterized by Θ, by minimising the squared loss function

$$\mathcal{L}(\Theta) := \frac{1}{2}\sum_{i=1}^{n} \|u(x_i) - y_i\|^2.$$

Under gradient flow, the evolution dynamics of the parameter during training is $\mathring{\Theta} = -\nabla_\Theta \mathcal{L}$ and, consequently, the evolution of the l-th component of network output $\boldsymbol{u}(x)$, for any input x, follows the differential equation

$$\begin{aligned}\mathring{u}_l(x) &= \left\langle \nabla_\Theta u_l(x), \mathring{\Theta} \right\rangle \\ &= -\sum_{i=1}^{n}\sum_{j=1}^{z} \langle \nabla_\Theta u_l(x), \nabla_\Theta u_j(x_i)\rangle \, (u_j(x_i) - y_{i,j}). \end{aligned} \tag{3}$$

While the above dynamics apparently involve interaction between the different dimensions of the output $u(x)$, through $\langle \nabla_\Theta u_l(x), \nabla_\Theta u_j(x_i)\rangle$, it is easy to observe that this interaction does not contribute to the dynamics of linear or kernel models. We formalise this in the following lemma.

Lemma 1 (**No interaction across output dimensions**). *Let $u : \mathbb{R}^d \to \mathbb{R}^z$ be either a linear model $u(x) = \Theta x$, or a kernel machine $u(x) = \Theta\psi(x)$, where ψ corresponds to the implicit feature map of a kernel k, that is, $k(x, x') = \langle \psi(x), \psi(x')\rangle$.*
Then in the infinite width limit ($h \to \infty$) the inner products between the gradients are given by

$$\langle \nabla_\Theta u_l(x), \nabla_\Theta u_j(x')\rangle = \begin{cases} 0 & \text{if } l \neq j, \\ x^\top x' & \text{if } l = j \text{ (linear case)}, \\ k(x, x') & \text{if } l = j \text{ (kernel case)}. \end{cases}$$

For infinite width neural networks, whose weights are randomly initialised with appropriate scaling, Jacot et al. (2018) show that at, initialisation, Lemma 1 holds with k being the neural tangent kernel. Approximations for wide neural networks further imply the kernel remains same during training (Liu et al., 2020), and so Lemma 1 continues to hold through training.

Remark 1 (**Multivariate regression = independent univariate regressions**). *A consequence of Lemma 1 is that the learning dynamics* (3) *simplifies to*

$$\mathring{u}_l(x) = -\sum_{i=1}^{n} \langle \nabla_\Theta u_l(x), \nabla_\Theta u_l(x_i)\rangle \, (u_l(x_i) - y_{i,l}),$$

that is, each component of the output u_l evolves independently from other $u_j, j \neq l$. Hence, one may solve a z-variate squared regression problem as z independent univariate problems. We discuss below that a similar phenomenon is true in SSL dynamics with disastrous consequences.

2.2 Dynamics of Näive SSL has Trivial Solution

We now present the learning dynamics of SSL with contrastive and non-contrastive losses in (1)–(2). For convenience, we first discuss the non-contrastive case. Assuming that the network function $u : \mathbb{R}^d \to \mathbb{R}^z$ is parametrised by Θ, the gradient of the loss $\mathcal{L}(\Theta) = \sum_{i=1}^{n} -u(x_i)^\top u(x_i^+)$ is

$$\nabla_\Theta \mathcal{L}(\Theta) = -\sum_{i=1}^{n}\sum_{j=1}^{z} u_j(x_i) \cdot \nabla_\Theta u_j(x_i^+) + u_j(x_i^+) \cdot \nabla_\Theta u_j(x_i)$$

Hence, under gradient descent $\mathring{\Theta} = -\nabla_\Theta \mathcal{L}$, the evolution of each component of $u(x)$, given by $\mathring{u}_l(x) = \left\langle \nabla_\Theta u_l(x), \mathring{\Theta} \right\rangle$ is

$$\mathring{u}_l(x) = \sum_{i=1}^{n} \sum_{j=1}^{z} \langle \nabla_\Theta u_l(x), \nabla_\Theta u_j(x_i) \rangle \, u_j(x_i^+) + \left\langle \nabla_\Theta u_l(x), \nabla_\Theta u_j(x_i^+) \right\rangle u_j(x_i). \tag{4}$$

Similarly, in the case of contrastive loss (1), the learning dynamics of $u(x)$, for any input x, is similarly expressed by

$$\begin{aligned} \mathring{u}_l(x) = \sum_{i=1}^{n} \sum_{j=1}^{z} & \langle \nabla_\Theta u_l(x), \nabla_\Theta u_j(x_i) \rangle \, u_j(x_i^+) + \left\langle \nabla_\Theta u_l(x), \nabla_\Theta u_j(x_i^+) \right\rangle u_j(x_i) \\ & - \langle \nabla_\Theta u_l(x), \nabla_\Theta u_j(x_i) \rangle \, u_j(x_i^-) - \left\langle \nabla_\Theta u_l(x), \nabla_\Theta u_j(x_i^-) \right\rangle u_j(x_i). \end{aligned} \tag{5}$$

We note Lemma 1 depends only on the model and not the loss function, and hence, it is applicable for the SSL dynamics in (4)–(5). However, there are no multivariate training labels $y \in \mathbb{R}^z$ in SSL (i.e. $y = 0$) that can drive the dynamics of the different components $u_1, \ldots, u_z$ in different directions, which leads to dimension collapse.

Proposition 1 (**Dimension collapse in SSL dynamcis**). *Under the conditions of Lemma 1, every component of the network output $u : \mathbb{R}^d \to \mathbb{R}^z$ has identical dynamics. As a consequence, the output collapses to one dimension at convergence.*
For linear model, $u(x) = \Theta x$, the dynamics of $u(x)$ is given by

$$\mathring{u}_l(x) = \sum_{i=1}^{n} (x^\top x_i) u_l(x_i^+) + (x^\top x_i^+) u_l(x_i)$$

for the non-contrastive case, and

$$\mathring{u}_l(x) = \sum_{i=1}^{n} (x^\top x_i) \big(u_l(x_i^+) - u_l(x_i^-) \big) + (x^\top x_i^+ - x^\top x_i^-) u_l(x_i)$$

for the contrastive case. For kernel models, the dynamcis is similarly obtained by replacing each $x^\top x'$ by $k(x, x')$.

By the extension of Lemma 1 to neural network and NTK dynamics, one can conclude that Proposition 1 and dimension collapse also happen for wide neural networks, when trained for the SSL losses in (1)–(2).

Remark 2 (**SSL dynamics for other losses**). *One may argue that the above dimension collapse is a consequence of loss definitions in* (1)–(2)*, and may not exist for other losses. We note that Liu et al. (2023) analyse contrastive learning with linear model under InfoNCE, and the simplified loss closely resembles* (1)*, which implies decoupling of output dimensions (and hence, dimension collapse) would also happen for InfoNCE. The same argument also holds for non-constrastive loss in Chen et al. (2020). However, for the spectral contrastive loss of HaoChen et al. (2021), the output dimensions remain coupled in the SSL dynamics due to existing interactions $u(x_i)^\top u(x_i^-)$ on the training data.*

Remark 3 (**Projections cannot overcome dimension collapse**). *Jing et al. (2022) propose to project the representation learned by a SSL model into a much smaller dimension, and show that fixed (non trainable) projectors may suffice. For a linear model, this implies $u(x) = A\Theta x$, where $A \in \mathbb{R}^{r \times z}, r \ll z$ is fixed. It is straightforward to adapt the dynamics and Proposition 1 to this case, and observe that for any $r > 1$, all the r components of $u(x)$ have identical learning dynamics, and hence, collapse at convergence.*

3 SSL with (Orthogonality) Constraints

For the remainder of the paper, we assume that the SSL model $u : \mathbb{R}^d \to \mathbb{R}^z$ corresponds to a 2-layer neural network of the form

$$x \in \mathbb{R}^d \xrightarrow{W_1} \mathbb{R}^h \xrightarrow{\phi(\cdot)} \mathbb{R}^h \xrightarrow{W_2^\top} u(x) = W_2^\top \phi(W_1 x) \in \mathbb{R}^z,$$

where h is the size of the hidden layer and $\Theta = (W_1, W_2^\top)$ are trainable matrices. Whenever needed, we use u^ϕ for the output to emphasize the nonlinear activation ϕ, and contrast it with a 2-layer linear network $u^{\mathbb{I}}(x) = W_2^\top W_1 x$.

Based on the discussion in the previous section, it is natural to ask how can the SSL problem be rephrased to avoid dimension collapse. An obvious approach is to add regularisation or constraints (Bardes et al., 2021; Ermolov et al., 2021; Caron et al., 2020). The most obvious regularisation or constraint on W_1, W_2 is entry-wise, such as on Frobenius norm. While there has been little study on various regularisations in SSL literature, a plethora of variants for Frobenius norm regularisations can be found for autoencoders, such as sum-regularsiation, $\|W_1\|_F^2 + \|W_2\|_F^2$, or product regularisation $\|W_2^\top W_1\|_F^2$ (Kunin et al., 2019).

It is known in the optimisation literature that regularised loss minimisation can be equivalently expressed as constrained optimisation problems. In this paper, we use the latter formulation for convenience of the subsequent analysis. The following result shows that Frobenius norm constraints do not prevent the output dimensions from decoupling, and hence, it is still prone to dimension collapse.

Proposition 2 (**Frobenius norm constraint does not prevent dimension collapse**). *Consider a linear SSL model $u^\phi(x) = W_2^\top \phi(W_1 x)$. The optimisation problem*

$$\begin{aligned} &\min_{W_1, W_2} \mathcal{L}(W_1, W_2) \\ &s.t. \quad \|W_1\|_F \leq c_1, \|W_2\|_F \leq c_2, \end{aligned}$$

where the loss $\mathcal{L}$ is given by (1) *or* (2)*, has a global solution $u(x) = [a(x)\ 0 \ldots 0]^\top \in \mathbb{R}^z$.*

The above result precisely shows dimension collapse for linear networks $u^{\mathbb{I}}$ even with Frobenius norm constraints. An alternative to Frobenius norm constraint can be to constrain the $L2$-operator norm. To this end, the following result shows that, for linear networks, the operator norm constraint can be realised in multiple equivalent ways.

Proposition 3 (**Equivalence of operator norm and orthonognality constraints**). *Consider a linear SSL model $u^{\mathbb{I}}(x) = W_2^\top W_1 x$, and let the loss $\mathcal{L}(W_1, W_2)$ be given by either* (1) *or* (2) *whose general form is $\mathcal{L}(W_1, W_2) = \left\|W_2^\top W_1 C W_1^\top W_2\right\|_2^2$, where C has atleast one negative eigenvalue. Then the following optimisation problems are equivalent:*

$$\begin{aligned} &1. \quad \min_{W_1, W_2} \frac{\mathcal{L}(W_1, W_2)}{\|W_2\|_2^2 \|W_1\|_2^2}; \\ &2. \quad \min_{W_1, W_2} \mathcal{L}(W_1, W_2) \quad s.t. \quad \|W_2\|_2 \leq 1,\ \|W_1\|_2 \leq 1; \\ &3. \quad \min_{W_1, W_2} \mathcal{L}(W_1, W_2) \quad s.t. \quad \|W_2^\top W_1\|_2 \leq 1; \\ &4. \quad \min_{W_1, W_2} \mathcal{L}(W_1, W_2) \quad s.t. \quad W_2^\top W_2 = \mathbb{I}_z,\ W_1^\top W_1 = \mathbb{I}_d. \end{aligned}$$

Additionally this regularization avoids dimension collapse.

Avoidance of dimensional collapse is also heuristically evident in the orthogonality constraint $W_2^\top W_2 = \mathbb{I}_z,\ W_1^\top W_1 = \mathbb{I}_d$, which we focus on in the subsequent sections. In particular we observe from the proof of Prop 3 that this regularization extracts the eigenvectors of C corresponding to its "most-negative" eigenvalues

Example 1 (**SSL dynamics on half moons**). *We numerically illustrate the importance of constraints in SSL. We consider a contrastive setting with the loss in* (1) *and $u(x) = W_2^\top \tanh(W_1 x)$ for the dataset shown in Figure 1a, where x^- is an independent sample from the dataset and $x^+ = x + \varepsilon$ where $\varepsilon \sim \mathcal{N}(0, 0.1\mathbb{I})$. Let us now compare the dynamics of $\mathcal{L}$ (no constraints) and $\mathcal{L}_{orth}$, the scaling loss that corresponds to orthogonality constraints, and present the results in Figure 1. We firstly observe in Figure 1a that the unconstrained loss does not converge. Secondly considering the embeddings as plotted in Figure 1b we observe dimension collapse for the unconstrained loss function (middle) but not for the one with orthogonal constraints (right).*

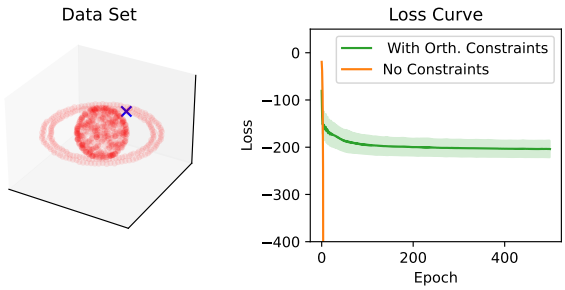

(a) Dataset and loss. **(left)** Illustration of the dataset in $\mathbb{R}^3$. The considered test point is marked with the blue cross. **(right)** Loss curve (mean over 100 initializations) for the network with and without orthogonal constraint.

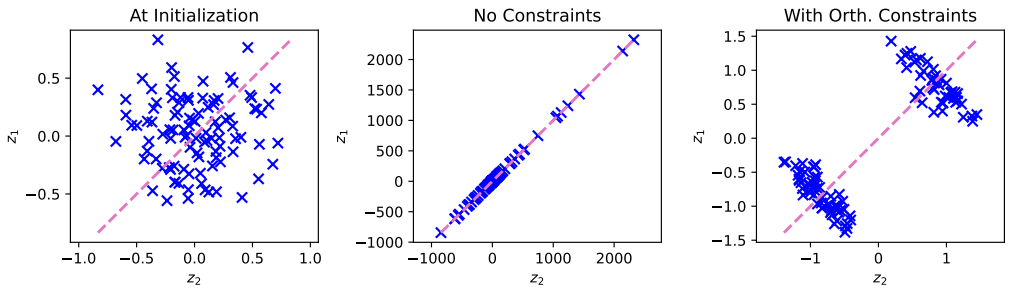

(b) Embedding into $\mathbb{R}^2$. **(left)** Embedding at initialization. **(middle)** Embedding for the network without constraints after 30 epochs. **(right)** Embedding for the network with orthogonal constraints after 500 epochs.

Figure 1: Illustration of dimension collapse. We consider the Dataset in Figure 1a and plot the loss for constraint and unconstrained models. In Figure 1b we furthermore plot the embedding at initialization and during training for both models.

3.1 Non-Linear SSL Models are Almost Linear

While the above discussion pertains to only linear models, we now show that the network, with nonlinear activation ϕ and orthognality constraints,

$$\begin{aligned} &u^{\phi}_{(t)}(x) = W_2^\top \phi(W_1 x) \\ &\text{s.t. } W_2^\top W_2 = \mathbb{I}_z,\ W_1^\top W_1 = \mathbb{I}_d, \end{aligned}$$

is almost linear. For this discussion, we explicitly mention the time dependence as a subscript $u^{\phi}_{(t)}$. We begin by arguing theoretically that in the infinite width limit at initialization there is very little difference between the output of the non-linear machine $u^{\phi}_{(0)}$ and that of its linear counterpart $u^{\mathbb{I}}_{(0)}$.

Theorem 1 (**Comparison of Linear and Non-linear Network**). *Recall that $u_{(t)}$ provides the output of the machine at time t and therefore consider the linear and non-linear setting at initialization as*

$$\begin{aligned} u^{\mathbb{I}}_{(0)} &= W_2^\top W_1 x && \text{s.t. } W_2^\top W_2 = \mathbb{I}_z,\ W_1^\top W_1 = \mathbb{I}_d; \\ u^{\phi}_{(0)} &= W_2^\top \phi\left(W_1 x\right) && \text{s.t. } W_2^\top W_2 = \mathbb{I}_z,\ W_1^\top W_1 = \mathbb{I}_d. \end{aligned} \tag{6}$$

Let $\phi(\cdot)$ be an activation function, such that $\phi(0) = 0$, $\phi'(0) = 1$, and $|\phi''(\cdot)| \leq c$. [3] *Then at initialization as uniformly random orthogonal matrices*

$$\left\| u^{\phi}_{(0)} - u^{\mathbb{I}}_{(0)} \right\| \ \leq\ Kc\,\|x\|^2\, d\sqrt{\frac{\log^4 h}{h}}$$

where K is an universal constant ϕ, d is the feature dimension and h the width of the hidden layer.

[3] This last assumption can also be weakened to say that ϕ'' is continuous at 0. See the proof of the theorem for details.

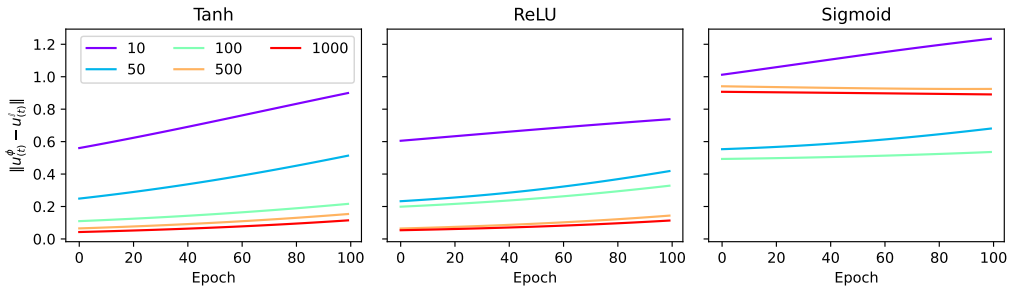

Figure 2: Difference between the non-linear output and the linear output under various conditions on the activation function. Change of the difference while training for hidden layer size 10 to 1000.

We furthermore conjecture that the same behaviour holds during evolution.

Conjecture 1 (**Evolution of Non-linear Networks**). *Consider the setup of Theorem 1 with the linear* $\left(u^{\mathbb{I}}_{(t)}\right)$ *and non-linear machine* $\left(u^{\phi}_{(t)}\right)$ *as defined in* (6) *and an optimization of the general*

$$\min_{W_2 W_1} \operatorname{Tr}\left(u_{(t)}^{\top} u_{(t)}\right)$$
$$\text{s.t.} \quad W_2^{\top} W_2 = \mathbb{I}_z \text{ and } W_1^{\top} W_1 = \mathbb{I}_d.$$

Again assume ϕ *is an activation function, such that* $\phi(0) = 0$ *and* $\phi'(0) = 1$. *Then*

$$\left\| u^{\phi}_{(t)} - u^{\mathbb{I}}_{(t)} \right\| \to 0 \quad \forall t > 0 \text{ as } h \to \infty.$$

Numerical justification of the above conjecture is presented in the following section.

3.2 Numerical Evaluation

We now illustrate the findings of of Theorem 1 and Conjecture 1 numerically. For evaluation we use the following experimental setup: We train a network with contrastive loss as defined in (1) using gradient descent with learning rate 0.01 for 100 epochs and hidden layer size from 10 to 1000. We consider the following three loss functions: (1) sigmoid, (2) ReLU ($\phi(x) = \max\{x, 0\}$) and (3) tanh. The results are shown in Figure 2 where the plot shows the average over 10 initializations. We note that *tanh* fulfills the conditions on ϕ and we see that with increasing layer size the difference between linear and non-linear goes to zero. While *ReLU* only fulfills $\phi(0) = 0$ the overall picture still is consistent with *tanh* but with slower convergence. Finally the results on *sigmoid* (which has a linear drift consistent with its value at 0) indicate that the conditions on ϕ are necessary as we observe the opposite picture: with increased layer width the difference between linear and non-linear increases.

4 Learning Dynamics of Linear SSL Models

Having showed that the non-linear dynamics are close to the linear ones we now analyze the linear dynamics. We do so by first showing that the two SSL settings discussed in the introduction can be phrased as a more general trace minimization problem. From there we derive the learning dynamics and discuss the evolution of the differential equation. Furthermore we numerically evaluate the theoretical results and show that the dynamics coincide with learning the general loss function under gradient decent.

We can define a simple linear embedding function u as: $u(x) = W_2^{\top} W_1 x$ where the feature dimension is d for n data points. The hidden layer dimension is h and embedding dimension z, such that the weights are

given by $W_2 \in \mathbb{R}^{h\times z}, W_1 \in \mathbb{R}^{h\times d}$. Therefore we can write our loss function as

$$\begin{aligned}\mathcal{L} &= \sum_{i=n}^{n} \operatorname{Tr}\left(W_2^\top W_1 x_i \left(x_i^- - x_i^+\right)^\top W_1^\top W_2\right) \\ &= \operatorname{Tr}\left(W_2^\top W_1 \widetilde{C} W_1^\top W_2\right) = \operatorname{Tr}\left(W_2^\top W_1 C W_1^\top W_2\right)\end{aligned}$$

with

$$C = \frac{\widetilde{C} + \widetilde{C}^\top}{2} \quad \text{and} \quad \widetilde{C} = \sum_{i}^{n} x_i \left(x_i^- - x_i^+\right)^\top. \tag{7}$$

Furthermore (1) can easily be extended to the p positive and q negative sample setting where we then obtain $\widetilde{C} = \sum_i^n \left(\sum_j^q x_i \left(x_j^-\right)^\top - \sum_j^p x_i \left(x_j^+\right)^\top\right)$. In addition we can also frame the previously considered non-contrastive model in (2) in the simple linear setting by considering the general loss function with $\widetilde{C} = \sum_i^n x_i \left(x_i^+\right)^\top$. We can now consider the learning dynamics of models, that minimize objects of the form

Definition 1 (General Loss Function)**.** *Consider the following loss function*

$$\begin{aligned}\mathcal{L}_{W_2W_1} &:= \operatorname{Tr}\left(W_2^\top W_1 C W_1^\top W_2\right) \\ \text{s.t.} \quad & W_2^\top W_2 = \mathbb{I}_z \text{ and } W_1^\top W_1 = \mathbb{I}_d.\end{aligned} \tag{8}$$

where $W_1 \in \mathbb{R}^{h\times d}$ and $W_2 \in \mathbb{R}^{h\times z}$ are the trainable weight matrices. $C \in \mathbb{R}^{d\times d}$ is a symmetric, data dependent matrix.

With the general optimization problem set up we can analyze (8) by deriving the dynamics under orthogonality constraints on the weights, which constitutes gradient descent on the Grassmannian manifold. While orthogonality constraints are easy to initialize the main mathematical complexity arises from ensuring that the constraint is preserved over time. Following Lai et al. (2020), we do so by ensuring that the gradients lie in the tangent bundle of orthogonal matrices.

4.1 Theoretical Analysis

In the following we present the dynamics in Theorem 2, followed by the analysis of the evolution of the dynamics in Theorem 3.

Theorem 2 (**Learning Dynamics in the Linear Setting**)**.** *Let us recall the the general linear trace minimization problem stated in* (8)*:*

$$\begin{aligned}&\min_{W_2W_1} \operatorname{Tr}\left(W_2^\top W_1 C W_1^\top W_2\right) \\ &\text{s.t.} \quad W_2^\top W_2 = \mathbb{I}_z \text{ and } W_1^\top W_1 = \mathbb{I}_d.\end{aligned}$$

where $W_1 \in \mathbb{R}^{h\times d}$ and $W_2 \in \mathbb{R}^{h\times z}$ are the trainable weight matrices and $C \in \mathbb{R}^{d\times d}$ a symmetric, data dependent matrices, such that $C = V\Lambda V^\top$ with $V := [v_1, \dots, v_d]$. Then with $q := \left[u^{\mathbb{I}}(v_1), \cdots, u^{\mathbb{I}}(v_d)\right]^\top$, where u represents the machine function i.e. $u^{\mathbb{I}}(x) = W_2^\top W_1 x$, the learning dynamics of q, the machine outputs are given by

$$\mathring{q} = -2\left[2\Lambda q - \Lambda q q^\top q - q q^\top \Lambda q\right]. \tag{9}$$

Similar differential equations to (9) have been analysed in Yan et al. (1994) and Fukumizu (1998). The typical way to find stable solutions to such equations involve converting it to a differential equation on $qq^\top$. This gives us a matrix riccati type equation. For brevity's sake we write below a complete solution when $z = 1$.

Evolution of the differential equation. While the above differential equation doesn't seem to have a simple closed form, a few critical observations can still be made about it - particularly about what this differential equation converges to. As observed in Figure 3 (right), independent of initialisation we converge to either of two points. In the following we formalise this observation.

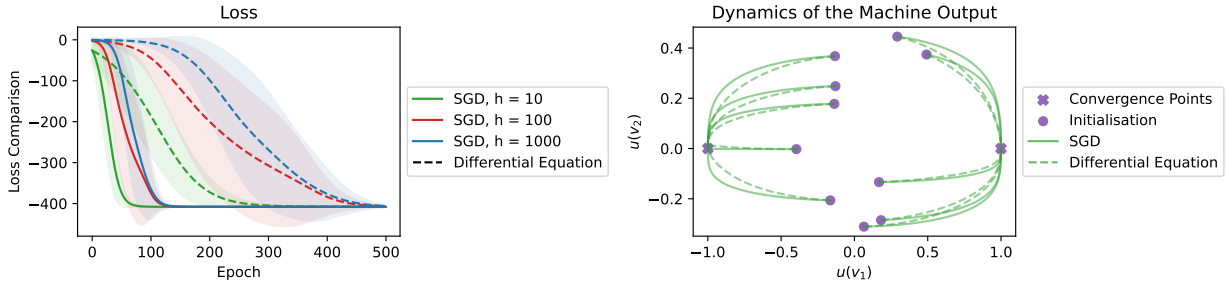

Figure 3: Comparison of gradient decent optimization and differential equation. **(left)** comparison of the loss function **(right)** comparison of the outputs.

Theorem 3 (Evolution of learning dynamics in (9) for $z = 1$)**.** *Let $z = 1$ then our update rule simplifies to*

$$\frac{\mathring{q}}{2} = -(1 - q^\top q)\Lambda q - (\mathbb{I} - qq^\top)\Lambda q. \tag{10}$$

We can distinguish two cases:

- *Assume all the eigenvalues of Λ are strictly positive then q converges to 0 with probability 1.*
- *Assume there is at least one negative eigenvalue of Λ, then q becomes the smallest eigenvector, v_1.*

The requirement of negative eigenvalues of C for a non-trivial convergence might be surprising however we can observe this when considering C in expectation. Let us assume C is constructed by (7) and note that $\mathbb{E}[\widetilde{C}] = \mathbb{E}\big[\sum_i^n x_i \left(x_i^- - x_i^+\right)^\top\big]$. While this already gives a heuristic of what is going on, for some more precise mathematical calculations, we can specialise to the situation where x^- is given by an independent sample and x^+ is given by adding a noise value ϵ sampled from $N(0, \sigma\mathbb{I})$, i.e. $x^+ = x + \epsilon$. Then

$$\mathbb{E}[\widetilde{C}] = \sum_{i=1}^n \mathbb{E}[x_i]\mathbb{E}[{x_i^-}^\top] - \mathbb{E}[x_i {x_i^+}^\top] = -n\mathbb{E}[xx^\top].$$

Thus $\mathbb{E}[C]$ is in fact negative definite. Extending Theorem 3 to a general $k > 1$ we conjecture the following to hold.

Conjecture 2. *If C has atleast k strictly negative eigenvalues and $v_1, ..., v_k$ are the eigenvectors corresponding to the most negative eigenvalues then the space spanned by $v_1, ..., v_k$ and that by $q_1, ..., q_k$ are the same in limit where q_i denotes the i'th column of q.*

We note that to prove the conjecture it is enough to show in limit $v_1, ..., v_k$ are each contained in the space spanned by $q_1, ..., q_k$. As the norm of v_i is 1, it is enough in turn to show that the norm of the projection of v_i onto the space of $q_1, ..., q_k$ converges to 1. We experimentally verify and illustrate this in Figure 5.

New Datapoint. While the above dynamics provide the setting during training we can furthermore investigate what happens if we input a new datapoint or a testpoint to the machine. Because u is a linear function and because $v_1, ..., v_d$ is a basis this is quite trivial. So if $\hat{x}$ is a new point, let $\alpha = (\alpha_1, ..., \alpha_d)^\top$ be the co-ordinates of $\hat{x}$, i.e. $\hat{x} = \sum_i^d \alpha_i v_i$ or $\alpha = V^\top \hat{x}$. Then

$$u_t(\hat{x}) = u_t\left(\sum_i^d \alpha_i v_i\right) = \sum_i^d \alpha_i u_t(v_i) = q_t^\top \alpha = q_t^\top V^\top \hat{x}.$$

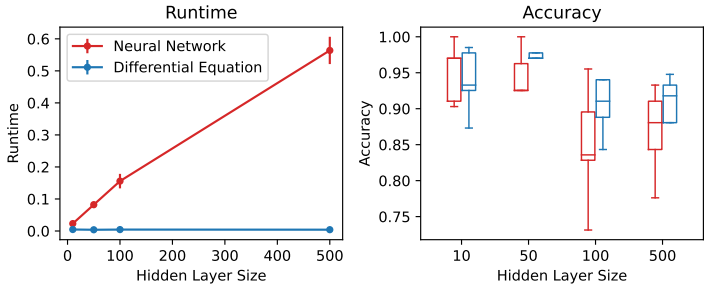

Figure 4: **(left)** Run-time comparison between running differential equation and SGD iteration for different hidden layer width. **(right)** Downstream task: Accuracy comparison for SVM on embedding obtained by SGD optimization and running the differential equation.

4.2 Numerical Evaluation

We can now further illustrate the above derived theoretical results empirically.

Leaning dynamics (Theorem 2) and new Datapoint. We can now illustrate that the derived dynamics in (9) do indeed behave similar to learning (8) using gradient decent updates. To analyze the learning dynamics we consider the gradient decent update of (8):

$$W_{1,2}^{(t+1)} = W_{1,2}^{(t)} + \eta \nabla \mathcal{L}_{W_2^{(t)}, W_1^{(t)}} \tag{11}$$

where $W_1^{(t)}, W_2^{(t)}$ are the weights at time step t and η is the learning rate as a reference. Practically the constraints in (8) are enforced by projecting the weights back onto $W_2^\top W_2 = \mathbb{I}_z$ and $W_1^\top W_1 = \mathbb{I}_d$ after each gradient step. Secondly we consider a discretized version of (9)

$$q_{t+1} = q_t - \eta\big[2\Lambda q_t - \Lambda q_t q_t^\top q_t - q_t q_t^\top \Lambda q_t\big]. \tag{12}$$

where q_t is the machine outputs at time step t. We now illustrate the comparison through in Figure 3 where we consider different width of the network ($h \in \{10, 100, 1000\}$) and $\eta = 0.01$. We can firstly observe on the left, that the loss function of the trained network and the dynamics and observe while the decay is slightly slower in the dynamics setting both converge to the same final loss value. Secondly we can compare the function outputs during training in Figure 3 (right): We initialize the NN randomly and use this initial machine output as q_0. We observe that during the evolution using (11) & (12) for a given initialization the are stay close to each other and converge to the same final outputs.

Numerical Evaluation of Theorem 3. We can again illustrate that the behaviour stated in Theorem 3 can indeed be observed empirically. This is shown in Figure 3 (right), a setting where C has negative eigenvalues. We observe that eventually the machine outputs converge to the smallest eigenvector.

Runtime and downstram task. Before going into the illustration of the dynamics we furthermore note that an update step using (12) is significantly faster then a SGD step using (11). For this illustration we now consider two classes with 200 datapoints each from the MNIST dataset Deng (2012). This is illustrated in Figure 4 (left) where we compare the runtime over different layer width (of which (12) is independent of). Expectantly (11) scales linearly with h and overall (12) has a shorter runtime per timestep. While throughout the paper we focus on the obtained embeddings we can furthermore consider the performance of downstream tasks on top of the embeddings. We illustrate this in the setting above where we apply a linear SVM on top of the embeddings. The results are shown in Figure 4 (right) where we observe that overall the performance of the downstream task for both the SGD optimization and the differential equation coincide.

Deep Linear Networks. Numerically we extend the illustration of the learning dynamics as derived in Theorem 2 for one hidden layer to multiple hidden layers. In Figure 6 we observe that for two and three hidden layer we still converge to the same final embedding as the one derived for one hidden layer.

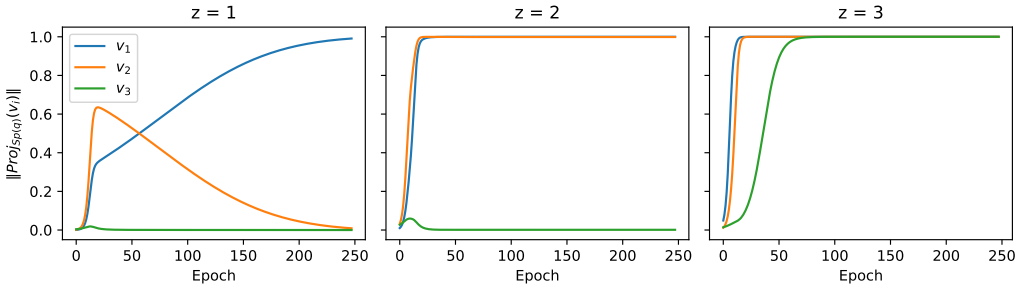

Figure 5: Consider the dataset presented in Figure 1a and embedding into $z = \{1, 2, 3\}$. Plotted is the norm of the projection of $v_1, \ldots v_3$ onto the space spanned by the collumns of q.

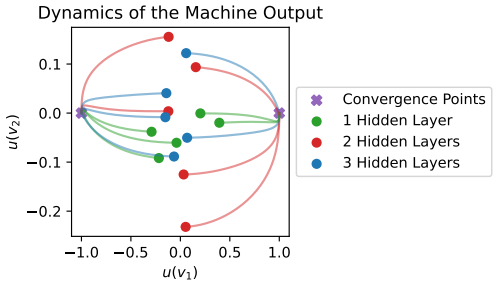

Figure 6: Numerical illustration of the convergence of deep linear models. We consider the same setting as considered above for the one hidden layer setting and plot similar dynamics for two and three hidden layer linear networks.

5 Conclusion

The study of learning dynamics of (infinite-width) neural networks has led to important results for the supervised setting. However, there is little understanding of SSL dynamics. Our initial steps towards analysing SSL dynamics encounters a hurdle: standard SSL training has drastic dimension collapse (Proposition 1), unless there are suitable constraints. We consider a general formulation of linear SSL under orthogonality constraints (8), and derive its learning dynamics (Theorem 2). We also show that the derived dynamics can approximate the SSL dynamics using wide neural networks (Theorem 1) under some conditions on activation ϕ. We not only provide a framework for analysis of SSL dynamics, but also shows how the analysis can critically differ from the supervised setting. As we numerically demonstrate, our derived dynamics can be used an efficient computational tool to approximate SSL models. In particular, the equivalence in Proposition 3 ensures that the orthogonality constraints can be equivalently imposed using a scaled loss, which is easy to implement in practice. We conclude with a limitation and open problem. Our analysis relies on a linear approximation of wide networks, but more precise characterisation in terms of kernel approximation (Jacot et al., 2018; Liu et al., 2020) may be possible, which can better explain the dynamics of deep SSL models. However, integrating orthogonality or operator norm constraints in the NTK regime remains an open question.

References

Sina Alemohammad, Zichao Wang, Randall Balestriero, and Richard G. Baraniuk. The recurrent neural tangent kernel. In *International Conference on Learning Representations*, 2021.

Sanjeev Arora, Simon S. Du, Wei Hu, Zhiyuan Li, Ruslan Salakhutdinov, and Ruosong Wang. On exact computation with an infinitely wide neural net. In *International Conference on Neural Information Processing Systems*, 2019a.

Sanjeev Arora, Hrishikesh Khandeparkar, Mikhail Khodak, Orestis Plevrakis, and Nikunj Saunshi. A theoretical analysis of contrastive unsupervised representation learning. In *International Conference on Machine Learning*, 2019b.

Randall Balestriero and Yann LeCun. Contrastive and non-contrastive self-supervised learning recover global and local spectral embedding methods. In *Advances in Neural Information Processing Systems*, 2022.

Yamini Bansal, Gal Kaplun, and Boaz Barak. For self-supervised learning, rationality implies generalization, provably. In *9th International Conference on Learning Representations*, 2021.

Han Bao, Yoshihiro Nagano, and Kento Nozawa. On the surrogate gap between contrastive and supervised losses. In *International Conference on Machine Learning*, 2022.

Adrien Bardes, Jean Ponce, and Yann LeCun. Vicreg: Variance-invariance-covariance regularization for self-supervised learning. *arXiv preprint arXiv:2105.04906*, 2021.

Jane Bromley, Isabelle Guyon, Yann LeCun, Eduard Säckinger, and Roopak Shah. Signature verification using a" siamese" time delay neural network. *Advances in neural information processing systems*, 1993.

Vivien Cabannes, Bobak Toussi Kiani, Randall Balestriero, Yann LeCun, and Alberto Bietti. The SSL interplay: Augmentations, inductive bias, and generalization. *CoRR*, abs/2302.02774, 2023.

Mathilde Caron, Ishan Misra, Julien Mairal, Priya Goyal, Piotr Bojanowski, and Armand Joulin. Unsupervised learning of visual features by contrasting cluster assignments. *Advances in neural information processing systems*, 2020.

Mathilde Caron, Hugo Touvron, Ishan Misra, Hervé Jégou, Julien Mairal, Piotr Bojanowski, and Armand Joulin. Emerging properties in self-supervised vision transformers. In *Proceedings of the IEEE/CVF International Conference on Computer Vision*, 2021.

Changyou Chen, Jianyi Zhang, Yi Xu, Liqun Chen, Jiali Duan, Yiran Chen, Son Tran, Belinda Zeng, and Trishul Chilimbi. Why do we need large batchsizes in contrastive learning? A gradient-bias perspective. In *Advances in Neural Information Processing Systems*, 2022.

Ting Chen, Simon Kornblith, Mohammad Norouzi, and Geoffrey Hinton. A simple framework for contrastive learning of visual representations. In *International conference on machine learning*. PMLR, 2020.

Xinlei Chen and Kaiming He. Exploring simple siamese representation learning. In *IEEE Conference on Computer Vision and Pattern Recognition*, 2021.

Yilan Chen, Wei Huang, Lam M. Nguyen, and Tsui-Wei Weng. On the equivalence between neural network and support vector machine. In *Advances in Neural Information Processing Systems 34*, 2021.

Li Deng. The mnist database of handwritten digit images for machine learning research. *IEEE Signal Processing Magazine*, 2012.

Jacob Devlin, Ming-Wei Chang, Kenton Lee, and Kristina Toutanova. BERT: pre-training of deep bidirectional transformers for language understanding. In *Proceedings of the 2019 Conference of the North American Chapter of the Association for Computational Linguistics: Human Language Technologies,*, 2019.

Simon S Du, Kangcheng Hou, Russ R Salakhutdinov, Barnabas Poczos, Ruosong Wang, and Keyulu Xu. Graph neural tangent kernel: Fusing graph neural networks with graph kernels. In *Advances in Neural Information Processing Systems*, volume 32, 2019.

Alan Edelman, Tomás A Arias, and Steven T Smith. The geometry of algorithms with orthogonality constraints. *SIAM journal on Matrix Analysis and Applications*, 1998.

Aleksandr Ermolov, Aliaksandr Siarohin, Enver Sangineto, and Nicu Sebe. Whitening for self-supervised representation learning. In *International Conference on Machine Learning*, 2021.

Basura Fernando, Hakan Bilen, Efstratios Gavves, and Stephen Gould. Self-supervised video representation learning with odd-one-out networks. In *IEEE conference on computer vision and pattern recognition*, 2017.

Kenji Fukumizu. Dynamics of batch learning in multilayer neural networks. In *ICANN 98: Proceedings of the 8th International Conference on Artificial Neural Networks*. Springer, 1998.

Jiawei Ge, Shange Tang, Jianqing Fan, and Chi Jin. On the provable advantage of unsupervised pretraining. *arXiv preprint*, abs/2303.01566, 2023.

Spyros Gidaris, Praveer Singh, and Nikos Komodakis. Unsupervised representation learning by predicting image rotations. *arXiv preprint arXiv:1803.07728*, 2018.

Jean-Bastien Grill, Florian Strub, Florent Altché, Corentin Tallec, Pierre H. Richemond, Elena Buchatskaya, Carl Doersch, Bernardo Ávila Pires, Zhaohan Guo, Mohammad Gheshlaghi Azar, Bilal Piot, Koray Kavukcuoglu, Rémi Munos, and Michal Valko. Bootstrap your own latent - A new approach to self-supervised learning. In *Advances in Neural Information Processing Systems*, 2020.

Lu Han, Han-Jia Ye, and De-Chuan Zhan. Augmentation component analysis: Modeling similarity via the augmentation overlaps. In *The Eleventh International Conference on Learning Representations*, 2023.

Jeff Z. HaoChen, Colin Wei, Adrien Gaidon, and Tengyu Ma. Provable guarantees for self-supervised deep learning with spectral contrastive loss. In *Advances in neural information processing systems*, 2021.

Reinhard Heckel and Fatih Furkan Yilmaz. Early stopping in deep networks: Double descent and how to eliminate it. In *International Conference on Learning Representations*, 2021.

Arthur Jacot, Franck Gabriel, and Clément Hongler. Neural tangent kernel: Convergence and generalization in neural networks. In *International Conference on Neural Information Processing Systems*, 2018.

Li Jing, Pascal Vincent, Yann LeCun, and Yuandong Tian. Understanding dimensional collapse in contrastive self-supervised learning. In *The Tenth International Conference on Learning Representations*, 2022.

Longlong Jing and Yingli Tian. Self-supervised visual feature learning with deep neural networks: A survey. *IEEE Transactions on Pattern Analysis and Machine Intelligence*, 2019.

Daniel D. Johnson, Ayoub El Hanchi, and Chris J. Maddison. Contrastive learning can find an optimal basis for approximately view-invariant functions. In *International Conference on Learning Representations*, 2023.

Angjoo Kanazawa, David W Jacobs, and Manmohan Chandraker. Warpnet: Weakly supervised matching for single-view reconstruction. In *IEEE Conference on Computer Vision and Pattern Recognition*, 2016.

Bobak Toussi Kiani, Randall Balestriero, Yubei Chen, Seth Lloyd, and Yann LeCun. Joint embedding self-supervised learning in the kernel regime. *CoRR*, abs/2209.14884, 2022. doi: 10.48550/arXiv.2209.14884.

Daniel Kunin, Jonathan Bloom, Aleksandrina Goeva, and Cotton Seed. Loss landscapes of regularized linear autoencoders. In *Proceedings of the 36th International Conference on Machine Learning*, 2019.

Zehua Lai, Lek-Heng Lim, and Ke Ye. Simpler grassmannian optimization, 2020. URL `https://arxiv.org/abs/2009.13502`.

Jason D. Lee, Qi Lei, Nikunj Saunshi, and Jiacheng Zhuo. Predicting what you already know helps: Provable self-supervised learning. In *Advances in Neural Information Processing Systems*, 2021.

Jiangyuan Li, Thanh V Nguyen, Chinmay Hegde, and Raymond K. W. Wong. Implicit sparse regularization: The impact of depth and early stopping. In *Advances in Neural Information Processing Systems*, 2021.

Chaoyue Liu, Libin Zhu, and Mikhail Belkin. On the linearity of large non-linear models: when and why the tangent kernel is constant. In *Advances in Neural Information Processing Systems 33*, 2020.

Ziyin Liu, Ekdeep Singh Lubana, Masahito Ueda, and Hidenori Tanaka. What shapes the loss landscape of self supervised learning? In *International Conference on Learning Representations*, 2023.

Ping Luo, Xinjiang Wang, Wenqi Shao, and Zhanglin Peng. Towards understanding regularization in batch normalization. In *International Conference on Learning Representations*, 2019.

Ishan Misra and Laurens van der Maaten. Self-supervised learning of pretext-invariant representations. In *Proceedings of the IEEE/CVF Conference on Computer Vision and Pattern Recognition*, 2020.

Abdel-Rahman Mohamed, Hung yi Lee, Lasse Borgholt, Jakob D. Havtorn, Joakim Edin, Christian Igel, Katrin Kirchhoff, Shang-Wen Li, Karen Livescu, Lars Maaløe, Tara N. Sainath, and Shinji Watanabe. Self-supervised speech representation learning: A review. *IEEE JSTSP Special Issue on Self-Supervised Learning for Speech and Audio Processing*, 2022.

Behnam Neyshabur, Srinadh Bhojanapalli, David McAllester, and Nati Srebro. Exploring generalization in deep learning. In *Advances in Neural Information Processing Systems*, 2017.

Thanh V. Nguyen, Raymond K. W. Wong, and Chinmay Hegde. Benefits of jointly training autoencoders: An improved neural tangent kernel analysis. *IEEE Transactions on Information Theory*, 2021.

David Novotny, Samuel Albanie, Diane Larlus, and Andrea Vedaldi. Self-supervised learning of geometrically stable features through probabilistic introspection. In *IEEE Conference on Computer Vision and Pattern Recognition*, 2018.

Arnu Pretorius, Steve Kroon, and Herman Kamper. Learning dynamics of linear denoising autoencoders. In *International Conference on Machine Learning*, 2018.

Mahalakshmi Sabanayagam, Pascal Esser, and Debarghya Ghoshdastidar. Representation power of graph convolutions : Neural tangent kernel analysis, 2022. URL `https://arxiv.org/abs/2210.09809`.

Nikunj Saunshi, Sadhika Malladi, and Sanjeev Arora. A mathematical exploration of why language models help solve downstream tasks. In *International Conference on Learning Representations*, 2021.

Andrew M. Saxe, James L. McClelland, and Surya Ganguli. Exact solutions to the nonlinear dynamics of learning in deep linear neural networks. In *International Conference on Learning Representations*, 2014.

Pierre Sermanet, Corey Lynch, Yevgen Chebotar, Jasmine Hsu, Eric Jang, Stefan Schaal, Sergey Levine, and Brain. Time-contrastive networks: Self-supervised learning from video. In *IEEE international conference on robotics and automation*, 2018.

Anshul Shah, Suvrit Sra, Rama Chellappa, and Anoop Cherian. Max-margin contrastive learning. In *AAAI Conference on Artificial Intelligence*, 2022.

Daniel Soudry, Elad Hoffer, Mor Shpigel Nacson, Suriya Gunasekar, and Nathan Srebro. The implicit bias of gradient descent on separable data. *Journal of Machine Learning Research*, 2018.

Steffen Steffen, Alexei Baevski, Ronan Collobert, and Michael Auli. wav2vec: Unsupervised pre-training for speech recognition, 2019.

Yuandong Tian. Understanding deep contrastive learning via coordinate-wise optimization. In *Advances in Neural Information Processing Systems*, 2022.

Christopher Tosh, Akshay Krishnamurthy, and Daniel Hsu. Contrastive learning, multi-view redundancy, and linear models. In *Algorithmic Learning Theory*, Proceedings of Machine Learning Research, 2021.

Aäron van den Oord, Yazhe Li, and Oriol Vinyals. Representation learning with contrastive predictive coding. *CoRR*, abs/1807.03748, 2018. URL `http://arxiv.org/abs/1807.03748`.

Colin Wei, Sang Michael Xie, and Tengyu Ma. Why do pretrained language models help in downstream tasks? an analysis of head and prompt tuning. In *Advances in Neural Information Processing Systems*, 2021.

Wei-Yong Yan, U. Helmke, and J.B. Moore. Global analysis of oja's flow for neural networks. *IEEE Transactions on Neural Networks*, 1994.

Runtian Zhai, Bingbin Liu, Andrej Risteski, Zico Kolter, and Pradeep Ravikumar. Understanding augmentation-based self-supervised representation learning via RKHS approximation. *CoRR*, abs/2306.00788, 2023.

Chiyuan Zhang, Samy Bengio, Moritz Hardt, Benjamin Recht, and Oriol Vinyals. Understanding deep learning requires rethinking generalization. In *International Conference on Learning Representations*, 2017.

Zhijian Zhuo, Yifei Wang, Jinwen Ma, and Yisen Wang. Towards a unified theoretical understanding of non-contrastive learning via rank differential mechanism. In *The Eleventh International Conference on Learning Representations*, 2023.

A Appendix

In the appendix we provide the following additional proofs

- Proof of Lemma1
- Proof of Proposition 2
- Proof of Proposition 3
- Proof of Theorem 1
- Proof of Theorem 2
- Proof of Theorem 3

A.1 Proof of Lemma1

Proof. Let the collumns of W_2 be denoted by $w_1, w_2, ..., w_z$. Then we note that each component of u, u_j is given by $u_j(x) = w_j^\top \phi(W_1 x)$. Thus if $l \neq j$, $u_j(x)$ has no dependence with w_l i.e. $\nabla_{w_l} u_j(x) = 0$. Thus we get that when $l \neq j$,

$$\langle \nabla_\Theta u_l(x), \nabla_\Theta u_j(x') \rangle = \langle \nabla_{W_1} u_l(x), \nabla_{W_1} u_j(x') \rangle .$$

We can now use Liu et al. (2020) (for instance its Lemma 3.1) which basically concludes that no training happens at the penultimate or prior layers. In limit all positive gradients arise only from the final layer. As such

$$\langle \nabla_{W_1} u_l(x), \nabla_{W_1} u_j(x') \rangle = 0.$$

By the same token, for $l = j$,

$$\begin{aligned} \langle \nabla_\Theta u_l(x), \nabla_\Theta u_j(x') \rangle &= \langle \nabla_{W_1} u_l(x), \nabla_{W_1} u_j(x') \rangle + \left\langle \nabla_{w_j} u_j(x), \nabla_{w_j} u_j(x') \right\rangle \\ &= \langle \phi(W_1 x), \phi(W_1 x') \rangle . \end{aligned}$$

Finally again using the fact that W_1 does not change in training and that W_1 is initialized from a normalized gaussian , when ϕ is the identity map, it is well known that the above converges to $x^\top x'$ (as there $\langle \phi(W_1 x), \phi(W_1 x') \rangle = x^\top (W_1^\top W_1) x \to x^\top x'$) and otherwise to a deterministic kernel k (see e.g. (Liu et al., 2020), (Arora et al., 2019b)). □

A.2 Proof of Proposition 2

Proof. For simplicity of the proof we begin by reformulating the loss function in both contrastive and noncontrastive setting to a more general form. In particular it is trivial to check that we can generalize by writing

$$\mathcal{L} = \mathrm{Tr}\left(W_2^\top f(X, W_1) W_2 \right),$$

where X denotes the collection of all the relevant data (i.e. $\forall\ 1 \leq i \leq n$ x_i, as well as x_i^+ and x^- where applicable), and $f(X, W_1) = \sum_{i=1}^n \phi(W_1 x_i) \left(\phi(W_1 x_i^-) - \phi(W_1 x_i^+) \right)^\top$ in the contrastive setting (equation 1) while $f(X, W_1) = -\sum_{i=1}^n \phi(W_1 x_i) \phi(W_1 x_i^+)^\top$ in the non-contrastive setting (equation 2.)

Then decompose

$$W_2 W_2^\top = \sum_{i=1}^k \sigma_i^2 v_i v_i^\top .$$

Note then that $\|W_2\|_F^2 = \text{Tr}\left(W_2 W_2^\top\right) = \sum_{i=1}^k \sigma_i^2$. Thus the optimization target,

$$\mathcal{L}(W_1, W_2) = \text{Tr}\left(W_2^\top f(X, W_1) W_2\right) = \text{Tr}\left(f(X, W_1) W_2 W_2^\top\right) = \text{Tr}\left(f(X, W_1) \sum_{i=1}^k \sigma_i^2 v_i v_i^\top\right)$$
$$= \sum_{i=1}^k \sigma_i^2 v_i^\top f(X, W_1) v_i \geq \min_{i=1 \ to \ k} \{v_i^\top f(X, W_1) v_i\} \sum_{i=1}^k \sigma_i^2 = \|W_2\|_F^2 \min_{i=1 \ to \ k} \{v_i^\top f(X, W_1) v_i\}.$$

Thus when the Frobenius norm is restricted (i.e. bounded between 0 and c), if $f(X, W_1)$ has atleast one negative eigenvalue the loss is minimized when v_1 is the eigenvector corresponding to the most negative eigenvalue of $f(X, W_1)$ with $\sigma_1 = \|W_2\|_F$, with no other non-zero singular value. On the other hand if $f(X, W_1)$ has no negative eigenvalue then the loss is minimized when $W_2 = 0$. □

A.3 Proof of Proposition 3

Proof. We begin by quickly observing that (1) $\iff$ (2). This is simply done by defining $\hat{W}_i = \frac{W_i}{\|W_i\|_2}$ for $i = 1, 2$. Then we have

$$\underset{W_1, W_2}{\text{argmin}} \frac{\text{Tr}\left(W_2^\top W_1 C W_1^\top W_2\right)}{\|W_1\|_2^2 \|W_2\|_2^2} = \underset{\hat{W}_1, \hat{W}_2 : \|\hat{W}_1\|_2 = \|\hat{W}_1\|_2 = 1}{\text{argmin}} \text{Tr}\left(\hat{W}_2^\top \hat{W}_1 C \hat{W}_1^\top \hat{W}_2\right)$$

Using the fact that at least one eigenvalue of C is strictly negative (this rules out the case that the optimal is achieved when $W_i = 0$ as that would have prevented division by norm) then we can quickly get that

$$\underset{\hat{W}_1, \hat{W}_2 : \|\hat{W}_1\|_2 = \|\hat{W}_1\|_2 = 1}{\text{argmin}} \text{Tr}\left(\hat{W}_2^\top \hat{W}_1 C \hat{W}_1^\top \hat{W}_2\right) = \underset{\hat{W}_1, \hat{W}_2 : \|\hat{W}_1\|_2 \leq 1; \|\hat{W}_1\|_2 \leq 1}{\text{argmin}} \text{Tr}\left(\hat{W}_2^\top \hat{W}_1 C \hat{W}_1^\top \hat{W}_2\right).$$

For (2) $\iff$ (3), we begin by observing that by submultiplicativity of norm, any W_1, W_2 such that $\|W_1\|_2 \leq 1$ and $\|W_2\|_2 \leq 1$ automatically falls is the optimization space given by $\left\|W_1^\top W_2\right\| \leq 1$ thus giving one direction of the optimization equivalence for free. For the other side we note that given any W_1, W_2 such that $\left\|W_1^\top W_2\right\|_2^2 = \left\|W_1^\top W_2 W_2^\top W_1\right\|_2 \leq 1$, we can construct $\hat{W}_1, \hat{W}_2$ such that $\left\|\hat{W}_i\right\| \leq 1$ and $W_1^\top W_2 W_2^\top W_1 = \hat{W}_1^\top \hat{W}_2 \hat{W}_2^\top \hat{W}_1$. This follows from considering the singular values decomposition of $W_1^\top W_2$, getting $W_1^\top W_2 = U^\top \Sigma V$. As the norm of the product is smaller than 1, all the entries of the singular value matrix Σ are less than 1. Thus depending upon which among d or z is larger we consider either the matrices ΣU and V or the matrices U and ΣV to be our candidate $\hat{W}_1$ and $\hat{W}_2$ respectively. To complete we will simply have to add zero rows to our choice i.e. say U and ΣV to match the dimensions (i.e. to get a $n \times d$ matrix from a $z \times d$ one).

Finally for (3) $\iff$ (4) we begin by defining $W = W_1^\top W_2$. Then the optimization problem in (3) becomes,

$$\min_{W : \|W\|_2 \leq 1} \text{Tr}\left(W^\top C W\right) = \min_{W : \|W\|_2 \leq 1} \text{Tr}\left(C W W^\top\right).$$

We then prove that we are done if we can prove the claim at optimal of (3) (i.e. the above optimization problem) all the eigenvalues of $WW^\top$ are 1 or 0. Given this claim the singular value decomposition of W becomes only $W = U^\top V$, where if $k = \textit{rank}(W)$, U is a $k \times d$ matrix and V a $k \times z$ matrix. Additionally by property of SVD, the collumns of U and V are orthonormal. Finally as

$$k = \textit{rank}(W) \leq \min\{\textit{rank}(W_1), \textit{rank}(W_2)\} \leq \min\{d, z\} \leq n,$$

we can add a bunch of zero rows to U and V to get our $n \times d$ and $n \times z$ matrices which will be our corresponding W_1 and W_2.

It remains to prove that $\text{Tr}\left(CWW^\top\right)$ is minimized when all the eigenvalues of $WW^\top$ are 1 or 0. To do this simply decompose

$$WW^\top = \sum_{i=1}^k \sigma_i^2 v_i v_i^\top,$$

where v_i is the set of orthonormal eigenvectors of $WW^\top$ corresponding to non-zero eigenvalues of $WW^\top$ (or alternatively non-zero singular values of W) Then

$$\begin{aligned}\operatorname{Tr}\left(CWW^\top\right) &= \operatorname{Tr}\left(C\sum_{i=1}^{k}\sigma_i^2 v_i v_i^\top\right)\\ &= \sum_{i=1}^{k}\sigma_i^2 \operatorname{Tr}\left(Cv_i v_i^\top\right)\\ &= \sum_{i=1}^{k}\sigma_i^2 v_i^\top C v_i.\end{aligned}$$

Thus if C has l many strictly negative eigenvalues $\lambda_1 \leq \cdots \leq \lambda_l$ with corresponding eigenvectors $c_1, \ldots, c_l$ and σ_i^2 is positive the above quantity is minimized by choosing as many of these as possible i.e. $v_1 = c_1, \ldots, v_{\min\{d,z,l\}} = c_{\min\{d,z,l\}}$ and setting the corresponding σ_i to be 1 while every setting all other eigenvalues to 0.

We then also note by consequence of the above proof that we avoid dimension collapse when possible i.e. when C has multiple strictly negative eigenvalues (which is what one should expect if the data is not one dimensional as $\mathbb{E}[C] = -\mathbb{E}[xx^\top]$) □

A.4 Proof of Theorem 1

Proof. Let us start by defining some properties for the non-linearity: Assume the non-linear function ϕ is continuously twice differentiable near 0 and has no bias i.e. $\phi(0) = 0$. Then via scaling we can assume WLOG that $\phi'(0) = 1$. As $|\phi''(x)| \leq c$, we get that [4]

$$|\phi(x) - x| \leq \frac{cx^2}{2}. \tag{13}$$

Recall that the mapping of the first weight matrix is given by $W_1 : \mathbb{R}^d \to \mathbb{R}^h, \quad h \gg d$ under the constraint that $W_1^\top W = \mathbb{I}$. Under uniformly random initialization by Lemma 2 (see proof below) then with probability asymptotically going to 1 we have that

$$\max\left(W_1\right)_{i,j}^2 \leq C\frac{\log^2 h}{h}$$

Thus the norm of each row of W_1 we get with a.w.h.p. :

$$\left\|\operatorname{row}_i\left(W_1\right)\right\|^2 = \sum_{j=1}^{d}(W_1)_{i,j}^2 \leq C\frac{d\log^2 h}{h}$$

From there we can now write the value of each node in the layer using Cauchy-Schwarz inequality as

$$\left|\operatorname{row}_i(W_1)\cdot x\right|^2 \leq \left\|\operatorname{row}_i\left(W_1\right)\right\|^2 \|x\|^2 \leq C\|x\|^2\frac{d\log^2 h}{h}. \tag{14}$$

We now apply the non-linearity to this quantity and denote the output of the first layer after the non-linearity as

$$v_i = \phi\left(\operatorname{row}_i\left(W_1\right)\cdot x\right)$$

Define the vector $\epsilon \in \mathbb{R}^h$, where

$$\epsilon_j = v_i - \operatorname{row}_i\left(W_1\right)\cdot x$$

[4] We can actually also use the weaker assumption that $\phi''(0)$ is continuous at 0. Thus there is some bounded (compact) set A containing 0 and a constant c such that $\forall x \in A$, $|\phi(x) - x| \leq \frac{cx^2}{2}$

Then we have for h large enough[5]:

$$\begin{aligned}
\|\epsilon\|^2 &= \sum_{i=1}^{h} \epsilon_i^2 \\
&= \sum_{i=1}^{h} (v_i - \mathrm{row}_i\left(W_1\right) \cdot x)^2 \\
&\leq \sum_{i=1}^{h} \frac{c^2}{4} \left(\mathrm{row}_i\left(W_1\right) \cdot x\right)^4 && \textit{by equation 13} \\
&\leq \sum_{i=1}^{h} \frac{c^2}{4} \left(C \|x\|^2 \frac{d \log^2 h}{h}\right)^2 && \textit{by equation 14} \\
&= K^2 c^2 \|x\|^4 \frac{h d^2 \log^4 h}{h^2} = K^2 c^2 \|x\|^4 \frac{d^2 \log^4 h}{h},
\end{aligned}$$

where K is the universal constant $\frac{C}{2}$. Combining this with the second layer we get the difference of the outputs of the two networks as

$$\begin{aligned}
\left\| u_{(0)}^{\phi} - u_{(0)}^{\mathbb{I}} \right\| &= \left\| W_2^\top v - W_2^\top W_1 x \right\| \\
&= \left\| W_2^\top \left(v - W_1 x\right) \right\| \\
&\leq \|W_2\| \|\epsilon\| = \|\epsilon\| && \textit{as } \|W_2\| = 1 \\
&\leq K c \|x\|^2 d \sqrt{\frac{\log^4 h}{h}} \\
&\to 0.
\end{aligned}$$

□

Lemma 2. *Given any $d \leq p$, Let Q be a uniformly random $h \times d$ semi-orthonormal matrix. I.e. Q is the first d columns of an uniformly random $h \times h$ orthonormal matrix. Then there are constants L and a sequence ϵ_p converging to 0 as h goes to infinity such that ,*

$$P\left(\max |Q_{i,j}| \geq \frac{L \log h}{\sqrt{h}}\right) \leq \epsilon_n$$

Proof. We note that it is enough to prove the claim when $d = h$, i.e. Q is uniformly random $h \times h$ orthonormal matrix. Then as our distribution is uniform, the density at any particular Q is same as the density at any UQ where U is some other fixed orthogonal matrix. Thus if q_1 is the first column of Q, the marginal distribution of q_1 has the property that its density at any q_1 is same as that of Uq_1 for any orthogonal matrix U. In other words the marginal distribution for any column of Q is simply that of the uniform unit sphere.

Consider then the following random variable which has the same distribution as that of a fixed column of Q i.e. uniform unit h-sphere. Let $X = (X_1, ..., X_h)$ be iid random variables from $\mathcal{N}(0, 1)$. Then we know that $X \sim \mathcal{N}(0, \mathbb{I}_h)$. From the rotational symmetry property of standard gaussian then we have that $\frac{X}{\|X\|}$ is distributed as an uniform sample from the unit sphere in h dimensions. By union bound then, we have

$$\begin{aligned}
P\left(\max_{1 \leq i \leq h} |X_i| \geq t \log h\right) &\leq \frac{1}{\sqrt{2\pi}} h e^{-\frac{t^2 \log^2 h}{2}} \\
\implies P\left(\max_{1 \leq i \leq h} |X_i| \leq t \log h\right) &\geq 1 - \frac{1}{\sqrt{2\pi}} h e^{-\frac{t^2 \log^2 h}{2}}.
\end{aligned}$$

[5]Note that for the weaker assumption we can still use equation 13. This is because by equation 14,w.h.p. $\mathrm{row}_i(W_1) \cdot x$ goes to 0 and thus $\mathrm{row}_i(W_1) \cdot x \in A$ in limit

As each X_i is iid normal, X_i^2 is iid Chi-square with $\mathbb{E}[X_i^2] = 1$, thus by Chernoff there exists constants C', c' such that

$$P\left(\frac{\sum_{i=1}^h X_i^2}{h} \geq 1 - s\right) \geq 1 - C'e^{-c'hs^2}.$$

Since $\max_{1\leq i\leq h}|X_i| \leq t\log h$ and $\frac{\sum_{i=1}^h X_i^2}{h} \leq (1+s)$ implies that $\max_{1\leq i\leq h}\frac{|X_i|}{\|X\|} \leq \frac{t\log h}{\sqrt{h(1-s)}}$, we get that

$$P\left(\max_{1\leq i\leq h}\frac{|X_i|}{\|X\|} \leq \frac{t\log h}{\sqrt{h(1-s)}}\right) \geq 1 - \frac{1}{\sqrt{2\pi}}he^{-\frac{t^2\log^2 h}{2}} - C'e^{-c'hs^2}$$

$$\implies P\left(\max_{1\leq i\leq h}\frac{|X_i|}{\|X\|} \geq \frac{t\log h}{\sqrt{h(1-s)}}\right) \leq \frac{1}{\sqrt{2\pi}}he^{-\frac{t^2\log^2 h}{2}} + C'e^{-c'hs^2}$$

From the argument before that any j'th column of Q is distributed as X. Using the above and another union bound then get us

$$P\left(\max_{1\leq i\leq h}\max_{1\leq i\leq h}|Q_{i,j}| \geq \frac{t\log h}{\sqrt{h(1-s)}}\right) \leq \frac{1}{\sqrt{2\pi}}he^{-\frac{t^2\log^2 h}{2}} + C'e^{-c'hs^2}$$

$$\implies P\left(\max_{1\leq j\leq h}\max_{1\leq i\leq h}|Q_{i,j}| \geq \frac{t\log h}{\sqrt{h(1-s)}}\right) \leq \frac{1}{\sqrt{2\pi}}h^2e^{-\frac{t^2\log^2 h}{2}} + C'he^{-c'hs^2}$$

We note that for any constants t, c' that as h goes to infinity, both $h^2e^{-\frac{t^2\log^2 h}{2}}$ and $he^{-c'hs^2}$ goes to zero. The proof is then finished by choosing some appropriate constants $s, t \geq 0$. □

A.5 Proof of Theorem 2

Proof. To simplify notation we are dropping the superscript $\mathbb{I}$ from $u^{\mathbb{I}}_{(t)}$. The u in the following proof is already presumed to be linear. For the same reason we are also dropping the symbol of time, t, from u, W_2, W_1 even though all of them are indeed time dependent. Finally for any time dependent function f, we denote $\frac{\partial f}{\partial t}$ by $\mathring{f}$.

From (Edelman et al., 1998), we get that the derivative of a function γ restricted to a grassmanian is derived by left-multiplying $1 - \gamma\gamma^\top$ to the "free" or unrestricted derivative of γ. Using this and recalling that the loss in Eq. 8 is given by

$$\mathcal{L} = \mathrm{Tr}\left(W_2^\top W_1 C W_1^\top W_2\right),$$

we therefore can write $\mathring{W}_1$ and $\mathring{W}_2$ as

$$\begin{aligned}
\mathring{W}_2(t) &= -\left(\mathbb{I} - W_2W_2^\top\right)\nabla_{W_2}\mathcal{L} = -2\left(\mathbb{I} - W_2W_2^\top\right)\left(W_1CW_1^\top W_2\right)\\
\mathring{W}_1(t) &= -\left(\mathbb{I} - W_1W_1^\top\right)\nabla_{W_1}\mathcal{L} = -2\left(\mathbb{I} - W_1W_1^\top\right)\left(W_2W_2^\top W_1C\right).
\end{aligned}$$

Thus we obtain

$$\begin{aligned}
\frac{\partial\, u_{(t)}(x)}{\partial\, t} =& \mathring{W}_2(t)^\top W_1(t)x + W_2(t)^\top \mathring{W}_1(t)x\\
=& \left(\left(\mathbb{I} - W_2W_2^\top\right)\left(-2W_1CW_1^\top W_2\right)\right)^\top W_1(t)x\\
&+ W_2(t)^\top\left(\mathbb{I} - W_1W_1^\top\right)\left(-2W_2W_2^\top W_1C\right)x\\
=& -2\left(W_2^\top W_1C\cancel{W_1^\top W_1}x \;+\; \cancel{W_2^\top W_2}W_2^\top W_1Cx\right)\\
&+ 2\left(W_2^\top W_1CW_1^\top W_2W_2^\top W_1x \;+\; W_2^\top W_1W_1^\top W_2\; W_2^\top W_1Cx\right)\\
=& -2\left(2W_2^\top W_1Cx - W_2^\top W_1CW_1^\top W_2W_2^\top W_1x \;-\; \sum_i^d W_2^\top W_1v_iv_i^\top W_1^\top W_2\; W_2^\top W_1Cx\right),
\end{aligned}$$

where we obtain the second equality by expanding the terms, taking advantage of $W_2^\top W_2 = \mathbb{I}, W_1^\top W_1 = \mathbb{I}$ and $\mathbb{I}_d = \sum_i^d v_i v_i^\top$. Now setting x as v_j and using the fact that they are eigenvectors for C and using $C = \sum_i^d \lambda_i v_i v_i^\top$ gives us:

$$\mathring{u}(v_j) = -2\left(2\lambda_j u_{(t)}(v_j) - \sum_i^d \lambda_i u_{(t)}(v_i) u_{(t)}(v_i)^\top u_{(t)}(v_j) - \lambda_j \sum_i^d u_{(t)}(v_i) u_{(t)}(v_i)^\top u_{(t)}(v_j)\right)$$

Let's rewrite this in matrix notation. First define $q := [u(v_1), \dots u(v_d)]^\top$ thus obtaining:

$$\mathring{q} = -2\big[2\Lambda q - \Lambda q q^\top q - q q^\top \Lambda q\big]$$

which concludes the proof. □

A.6 Proof of Theorem 3

Proof. For instance first suppose that all the eigenvalues of Λ are strictly positive and thus $q^\top \Lambda q > 0$. Then

$$\begin{aligned}\frac{d(q^\top q)}{dt} &= 2q^\top \mathring{q} = 4\big[-(1-q^\top q)q^\top \Lambda q - q^\top(\mathbb{I} - qq^\top)\Lambda q\big] \\ &= -8(1-q^\top q)q^\top \Lambda q\end{aligned}$$

Observing now that because of orthonormality of our weight matrices, $q^\top q = \|q\|^2 < 1$ (as $\|q\| \neq 1$ at initialization with probability 1) we get that the derivative of $\|q\|^2$ is always negative and thus q converges to 0.

Now suppose on the other hand there is atleast one negative eigenvalue. WLOG let e_1 denote the eigenvector with the smallest eigenvalue (which is negative). Then

$$\begin{aligned}\frac{d(e_1^\top q)}{dt} &= e_1^\top \mathring{q} = 2\big[-(1-q^\top q)e_1^\top \Lambda q - e_1^\top(\mathbb{I} - qq^\top)\Lambda q\big] \\ &= 2\big[(1-q^\top q)(-\lambda_1)e_1^\top q + (q^\top \Lambda q - \lambda_1)e_1^\top q)\big]\end{aligned}$$

We now note that $q^\top \Lambda q - \lambda_1 \geq 0$ as λ_1 is the smallest eigenvalue. Thus as $-\lambda_1$ is positive, the derivative of $e_1^\top q$ is always positive unless $1 - q^\top q = q^\top \Lambda q - \lambda_1 = 0$, which only happens at $q = e_1$. In other words, eventually q becomes the smallest eigenvector e_1. □